

Applicability of a Conservative Margin Approach for Assessing NDE Flaw Detectability

Ajay M. Koshti, NASA Johnson Space Center

Abstract

Nondestructive Evaluation (NDE) procedures are required to detect flaws in structures with a high percentage detectability and high confidence. Conventional Probability of Detection (POD) methods are statistical in nature and require detection data from a relatively large number of flaw specimens. In many circumstances, due to the high cost and long lead time, it is impractical to build the large set of flaw specimens that is required by the conventional POD methodology. Therefore, in such situations it is desirable to have a flaw detectability estimation approach that allows for a reduced number of flaw specimens but provides a high degree of confidence in establishing the flaw detectability size. This paper presents an alternative approach called the conservative margin approach (CMA). To investigate the applicability of the CMA approach, flaw detectability sizes determined by the CMA and POD approaches have been compared on actual datasets. The results of these comparisons are presented and the applicability of the CMA approach is discussed.

Introduction

It is essential to estimate NDE flaw detectability for any given application. The NDE procedure is required to detect flaws larger than or equal to a specific flaw size dictated by the engineering, called the requirement flaw size a_r , with a high percentage detectability and high confidence. The NDE flaw detectability can be given as the flaw size denoted as $a_{90/95}$ using the Probability of Detection (POD) curve fit method. The subscript indicates 90% POD with 95% lower confidence bound. Typically, $a_{90/95}$ is required for inspection of critical parts. The $a_{90/95}$ size may be influenced by the sample size in the NDE trials data. Flaw sizes with less confidence e.g. $a_{90/50}$ may be used for non-critical parts. The $a_{90/50}$ size is also known as the best fit estimate from the POD(a) curve with POD of 90%. It is less influenced by the sample size of the NDE trials data and is supported by a goodness of fit measure to the POD(a) curve. The $a_{90/95}$ size is based on estimating 95% confidence bound on the POD(a) curve.

Here, we seek to estimate flaw detectability a_d using a few NDE trial outcomes data based on modeling the best fit or best estimate POD(a) curve. We will not address a comparison of flaw detectability a_d with $a_{90/95}$ size in order to keep our objective less complex. Instead we seek to provide a positive margin to the unknown flaw size $a_{90/50}$. Thus, we seek the flaw detectability size a_d to be an estimate of $a_{90/50}$. CMA uses similarity with existing POD data sets. A typical POD(a) curve is shown in Fig. 1. One of the common software tools used in POD analysis is listed in Ref. 1. MIL-HDBK-1823 provides information on the POD(a) curve fit methods². Berens³ provides an overview of POD methods. The NTIAC NDE data⁴ provides POD estimation on many real data sets.

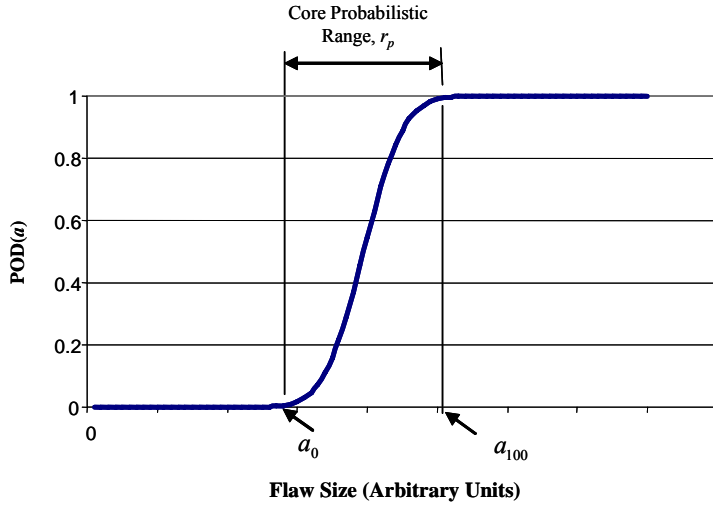


Figure 1: Typical Shape of a $POD(a)$ Curve

Threshold Flaw Sizes a_0 and a_{100}

The CMA models the $POD(a)$ curve as a straight line between two points e.g. adjusted a_0 ($POD(a_0) = 0$) and adjusted a_{100} ($POD(a_{100}) = 100\%$) shown in Fig. 1. An example of the NDE outcomes data from an NDE flaw detection experiment on many flaw specimens is provided in Fig. 2 to illustrate definitions of flaw sizes a_0 and a_{100} . The triangles indicate fraction of flaws detected. The data shows that, above a certain upper threshold for the flaw size (denoted as a_{100}), the observed flaw detectability is 100%. We are extremely interested in this flaw size as it can be used in the CMA.

In this example, a straight line is drawn to establish a boundary of the observed flaw detectability from low to high values of the observed flaw detectability. The intersection of the line with 100% flaw detectability level in the data could be considered to be one of the estimates of the upper threshold flaw size (a_{100}). The estimate could be viewed as the “upper knee point” in the data. Similarly, we can find the smallest flaw size above which the observed flaw detectability is 100%. This size is another estimate of a_{100} and is illustrated in Fig. 2. The estimate could be viewed as the “observed” upper threshold in the data. The flaw size $a_{90/50}$ can be considered to be the flaw size a_{100} . Note that the three estimates of the upper threshold size are very close to each other in this example.

Similarly, a lower threshold for the flaw size, denoted by a_0 , below which the observed flaw detectability is zero, can be defined. The lower threshold may be defined in terms of POD too. The lower threshold size can be defined as a flaw size with a $POD(a)$ of 10%. A region of flaw sizes between a_0 and a_{100} where the flaw detectability is strongly dependent on the flaw size and the observed flaw detectability values are between 0% and 100%, is defined as the core probabilistic range r_p .

$$r_p = a_{100} - a_0 \quad (1)$$

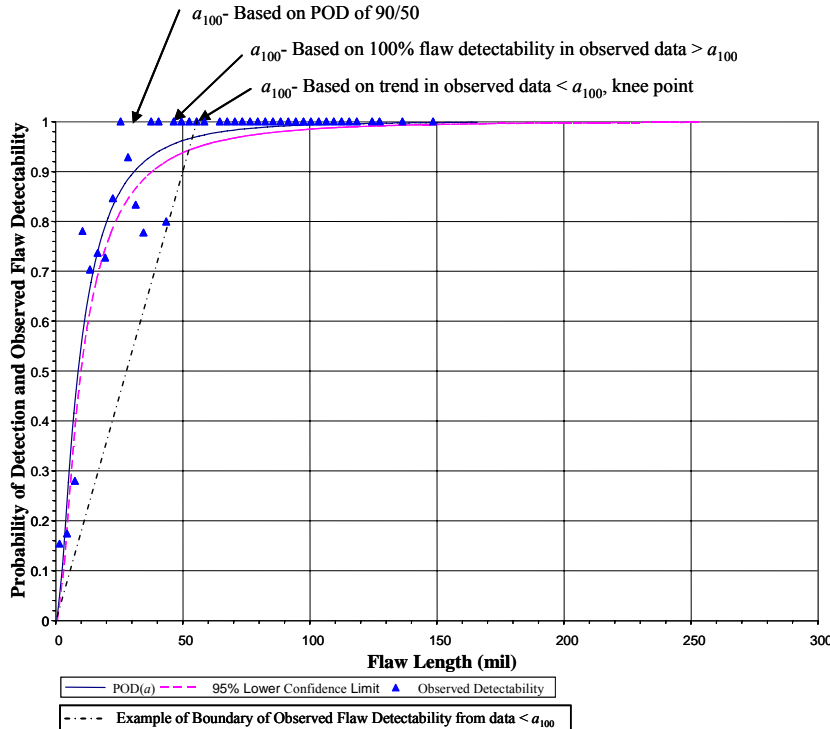


Figure 2: An Example of POD Data from NDE Trials

Formulation of Conservative Margin Approach (CMA)

The CMA estimate of flaw detectability is given by,

$$a_d = a_{100} + m. \quad (2)$$

The margin m seeks to account for uncertainty in a_{100} due to smaller sample size and seeks to establish a desirable positive margin from $a_{90/50}$. Here, we define the conservative margin Δ_1 as a measure of success for the CMA when compared with $a_{90/50}$ of an NDE outcomes dataset.

$$\Delta_1 = a_d - a_{90/50} \quad (3)$$

If the margin is positive and reasonable (e.g. $> 10\%$) for all possible estimates of CMA, then the CMA has demonstrated its applicability for the data set used or for the NDE techniques that can be assumed to have similar $POD(a)$ curve characteristics (such as β explained later).

The margin m is computed by modeling the $POD(a)$ curve by a straight line from the adjusted a_0 ($POD(a_0) = 0$) and adjusted a_{100} ($POD(a_{100}) = 100$). In order to use the CMA, it is necessary to verify the assumption of improvement in flaw detectability with flaw size. Ideally, the CMA should be validated based on comparison to the applicable POD analysis. It assumes that the best fit $POD(a)$ curve for the NDE process has a sharp upper knee which is defined as portion of the $POD(a)$ curve with POD between 90% and 97.6%. Note that, if Binomial distribution is applicable then $a_{90/95} \approx a_{97.6/50}$.

This technique assumes that a_0 and a_{100} can be clearly identified as smallest flaw detected and largest flaw missed respectively. Such a data can be called as a regular or non-contaminated

data. In some situations, the data does not have a clear a_0 and a_{100} due to non-detection of very large flaws. The non-detection of large flaws (size $\gg a_{90/50}$) is considered to be “irregular data” with outlier data points as they may not conform to a single mode mathematical distribution which is the basis for POD analysis. The existence of the outlier data points is commonly justified by NDE practitioners by statement that “not all flaws are created equal”. The $POD(a)$ curve for such a dataset usually does not have a sharp knee and it may be impossible to locate a_{100} . The $POD(a)$ curve fit method is the only method that can be used in this situation. Regular POD distributions with sharp upper knee are desirable for CMA. If a distribution has a sharp upper knee, then the $POD(a)$ curve in the core probabilistic range can be approximated by a straight line used in the CMA method. Thus, the knowledge of the shape of $POD(a)$ curve based on the similarity to an existing NDE outcomes datasets is essential to make the determination that the NDE technique provides a “regular” data set with a sharp knee so that a_{100} and $a_{90/50}$ are close.

It is assumed that uncertainty in the estimation of a_{100} and a_0 for a_0 is inevitable due to limited sample size. The uncertainty in a_{100} is compensated by a factor called k_U or the k -factor. The value of k -factor is dependent upon the number of flaws at a_{100} used to determine the size. A minimum sample size of 5 flaws at the suspected size a_{100} is recommended in determination of the a_{100} . The value of k -factor is calculated as

$$k_U = 1.0 - \hat{p}_L, \text{ where, } \frac{n_d}{n} = 1.0 \text{ and LCL} = 95\%, \quad (4)$$

where \hat{p}_L = the Binomial estimation of probability with LCL = 95%. Fig. 3 provides a plot of the k -factor as a function of the sample size of flaws with the size equal to a_{100} . n_d = number of flaws detected, n = total number of flaws. Table 1 provides the values of the k -factor.

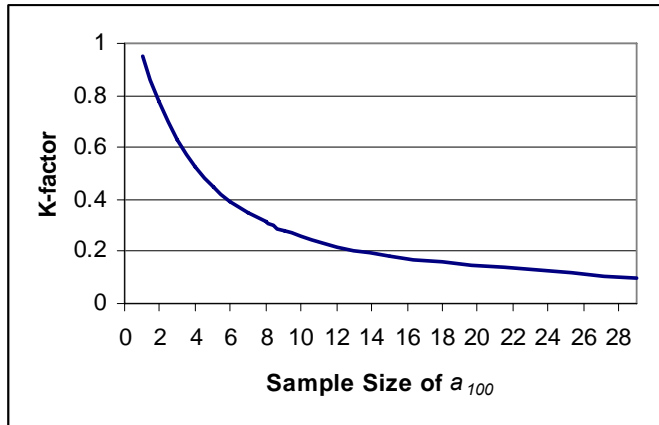


Figure 3: Minimum Values of k-factor for $\frac{n_d}{n} = 1.0$

The compensated a_{100} is given by,

$$a_{100}^c = a_{100} + jr_p k_U. \quad (5)$$

Here j (≥ 0) is introduced to control the amount of compensation. Similarly, the uncertainty in a_0 is compensated by a factor called k_L . The value of this k -factor is dependent upon the number of flaws at a_0 used to determine the size. A minimum sample size of 5 flaws at the suspected size a_0 is recommended in determination of the a_0 .

n	K-factor	q (j = 0.5)	q (j = 1)
4	0.53	1.67	1.81
5	0.45	1.33	1.65
6	0.39	1.27	1.55
7	0.35	1.24	1.47
8	0.31	1.21	1.41
9	0.28	1.18	1.36
10	0.26	1.16	1.32
11	0.24	1.15	1.29
12	0.22	1.13	1.27
13	0.20	1.12	1.25
14	0.19	1.11	1.23
15	0.18	1.11	1.21
16	0.17	1.10	1.20
17	0.16	1.09	1.19
18	0.15	1.09	1.18
19	0.15	1.08	1.17
20	0.14	1.08	1.16
21	0.13	1.08	1.15
22	0.13	1.07	1.14
23	0.12	1.07	1.14
24	0.12	1.07	1.13
25	0.11	1.06	1.12
26	0.11	1.06	1.12
27	0.11	1.06	1.12
28	0.10	1.06	1.11
29	0.10	1.06	1.11

Table 1: k -Factor and a_{100} Multiplier $q_{a_0=0}$

The value of k -factor is calculated as

$$k_L = \hat{p}_U, \text{ where, } \frac{n_d}{n} = 0.0 \text{ and UCL} = 95\%, \quad (6)$$

where, \hat{p}_U = the Binomial estimation of probability with UCL = 95%. The two k -factors (eqs. (4) and (6)) provide the same value for the same value of n . $k_L = k_U = k$ if the same number of flaws are used to determine a_0 and a_{100} . Therefore, Fig. 3 and Table 1 are applicable for both k -factors. The compensated a_0 is given by,

$$a_0^c = a_0 - jr_p k_L, \text{ where } a_0^c \geq 0, \text{ else } a_0^c = 0. \quad (7)$$

Note that flaw size a_0^c can not be negative. From eq. (7), $a_0^c > 0$ implies $a_0 \geq jr_p k_L$.

The compensated probabilistic range is given by,

$$r_p^c = a_{100}^c - a_0^c, \quad \text{where } a_0^c \geq 0. \quad (8)$$

Substituting eqs. (5) and (7), we get,

$$r_p^c = a_{100} - a_0 + jr_p k_U + jr_p k_L, \text{ where } a_0 \geq jr_p k_L. \quad (9)$$

After substituting eq. (1) and simplifying we get,

$$r_p^c = (1 + j(k_U + k_L))r_p \quad a_0 \geq jr_p k_L. \quad (10)$$

Here, we define the expression in the parenthesis as a range compensation factor k_r . Thus,

$$k_r = (1 + j(k_U + k_L)) \quad a_0 \geq jr_p k_L. \quad (11)$$

The compensated range is given by,

$$r_p^c = k_r r_p. \quad (12)$$

Here, we introduce a term l defined as ratio of the threshold sizes.

$$l = \frac{a_0}{a_{100}}, \quad 0 < l < 1. \quad (13)$$

Therefore, the range can be expressed as

$$r_p = (1-l)a_{100}. \quad (14)$$

From eq. (7) it can be shown that, $a_0 \geq jr_p k_L$ is equivalent to $(1+jk_L)(1-l) \leq 1$.

Therefore, eq. (12) can be written as,

$$r_p^c = (1+j(k_U + k_L))(1-l)a_{100}, \text{ for } (1+jk_L)(1-l) \leq 1. \quad (19a)$$

Hence, the condition on k_r can be expressed as,

$$k_r = (1+j(k_U + k_L)), \text{ for } (1+jk_L)(1-l) \leq 1. \quad (19b)$$

If this condition is not met i.e. $(1+jk_L)(1-l) > 1$, then we assume $a_0 = 0$. $a_0 = 0$ implies that $l = 0$ and we simplify eq. (10) as follows.

$$r_p^c = (1+jk_U)a_{100}, \quad \text{for } (1+jk_L)(1-l) > 1, a_0 = 0. \quad (20a)$$

Thus, here is another expression of k_r if $a_0 = 0$.

$$k_r = (1+jk_U), \quad \text{for } (1+jk_L)(1-l) > 1, a_0 = 0. \quad (20b)$$

The margin is calculated as,

$$m = r_p^c k_U. \quad (21)$$

The above equation implies that the margin is calculated by proportioning the compensated range by k -factor k_U . The above equation can also be written as,

$$m = k_r r_p k_U. \quad (22)$$

Eq. (2) can be written as,

$$a_d = qa_{100}, \quad (23)$$

where, q is defined as a multiplier to a_{100} or coefficient of a_{100} to estimate a_d . By manipulating Eqs. (2), (14) and (22), we can derive the following expression from q .

$$q = 1 + k_r(1-l)k_U. \quad (24)$$

Substituting the expressions for k_r from eqs. (19b) and (20b) we get,

$$q = 1 + (1+j(k_U + k_L))(1-l)k_U \quad \text{for } (1+jk_L)(1-l) \leq 1, \quad (25)$$

and

$$q_{a_0=0} = 1 + (1+jk_U)k_U \quad \text{for } (1+jk_L)(1-l) > 1, a_0 = 0. \quad (26)$$

Eq. (26) is the short expression for q compared to eq. (25). These two equations are needed to compute a_d . Fig. 4 illustrates the concept of CMA.

If we do not have enough data to estimate a_0 , it may be assumed to be zero. It will yield a more conservative estimate of a_d , provided data points for a_{100} are same in both cases.

$$q_{a_0=0} \geq q \quad (27)$$

The effort required to determine a_0 experimentally may not provide adequate payback in terms of improving estimate of a_d . Therefore, in most situations it is practical to assume that $a_0 = 0$ and only determine the size a_{100} experimentally. Eq. (27) allows us to make this simplification. Elimination of experimental determination of a_0 , makes the CMA approach attractive for

implementation as only a few flaws are needed to determine flaw detectability size a_d . The computation of $q_{a_0=0}$ only requires that the j factor accounts for the uncertainty in the range at the upper end only as opposed to using the same j value for compensation at lower end of the range in computation of the multiplier q . The simplification probably allows better correlation between j and the conservative margin for $q_{a_0=0}$.

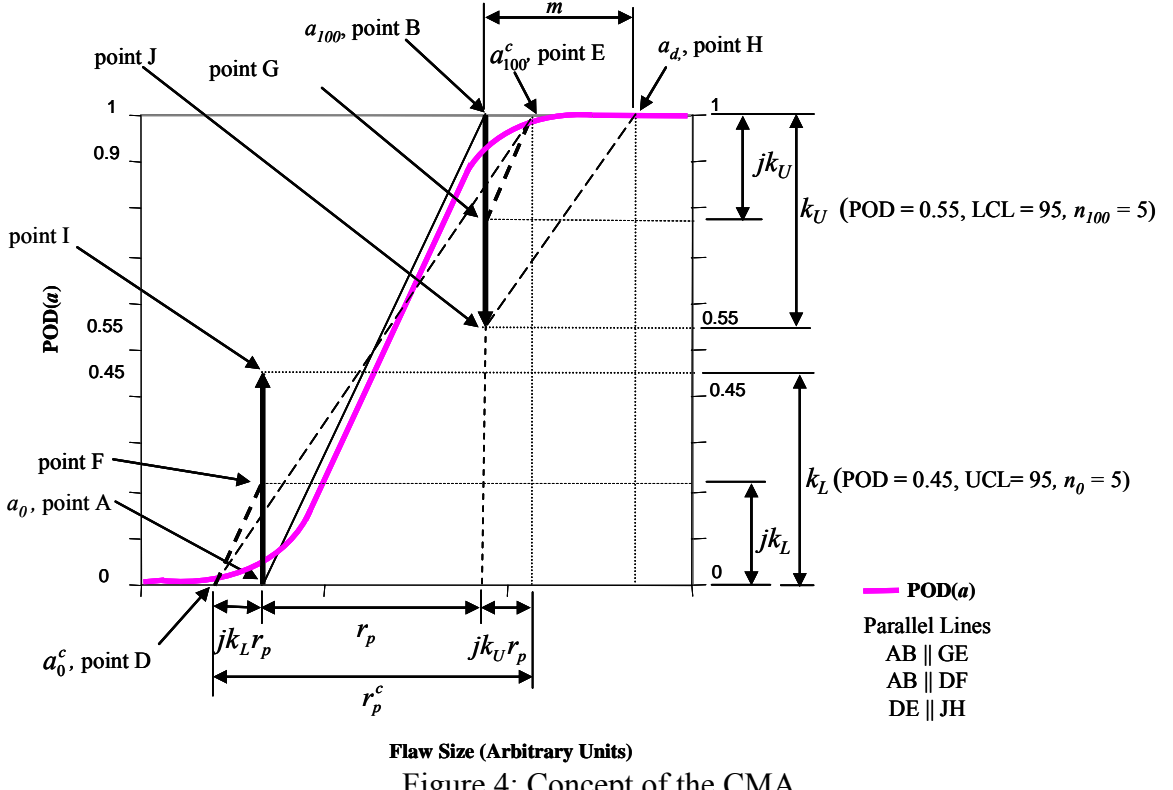


Figure 4: Concept of the CMA

The value of j is proposed to be between 0 and 1. We compensate for uncertainty in the range using the values of k -factors separately and then multiply the compensation factors. This may result in overcompensation. The compensation factors should account for the sharpness of the knees in the unknown $POD(a)$ curve. Choice of j value allows us to adjust conservatism in our calculation. Higher values of j would increase the value of q . Values of q for $a_0 = 0$ are given in Table 1. These values are plotted in Fig. 5. Examining these values, we conclude that we have assumed that a_{100} is not underestimated by more than 50% so that a_d may be approximately twice as much as a_{100} . Later, we would analyze some NDE data to compare results which may provide pointers for choosing values of j .

Eqs. (25) and (26) are plotted in Fig. 5 for $j = 1$. Fig. 5 indicates that q can be as high as 1.8. q decreases with a sample size n . It also decreases slightly with the ratio l . It is common practice among NDE practitioners to quote NDE flaw detectability to be twice the detectability demonstrated on a small number of flaws. The CMA is no exception to that rule.

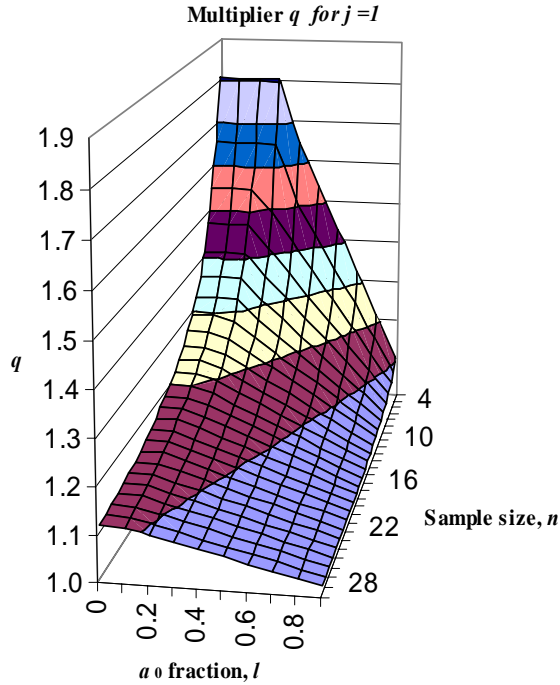


Figure 5: q Plotted against a_0 Fraction and Sample Size for $j = 1$

Use of Similarity of Existing POD Data for Qualifying CMA

Although, only a few flaws are needed to establish a_{100} and to compute the a_d , there are certain conditions that need to be met before the CMA equations can be used. Even if the $POD(a)$ curve for the NDE application of concern is not known, we assume certain characteristics of the unknown $POD(a)$ curve based on the similarity between the application of concern and a similar application with existing data and $POD(a)$ curve. The similarity can be established by studying certain characteristics of a family of $POD(a)$ curves belonging to the applicable method/technique. The study may reveal a range of characteristics of the $POD(a)$ curves within the family. The similarity study then may allow us to locate the NDE application of concern within the family of similar NDE method/techniques with available $POD(a)$ curve data.

The CMA approach can be validated on the family of NDE method/techniques by comparing the results of CMA with the known $a_{90/50}$ within the family of the method/techniques. Once, the CMA is validated for a family of NDE applications, it can be used for an application of concern belonging to the same family based on the similarity. The validation involves computing the conservative margin for many estimates of CMA with values of j established by trial and error so that a minimum desirable conservative margin is demonstrated. The methodology is discussed below by using two examples.

Here, we consider two examples to illustrate and specify the conditions on the slope of the assumed $POD(a)$ curve. The following data (Fig. 6) was taken from the NTIAC⁴ Data book.

Example 1

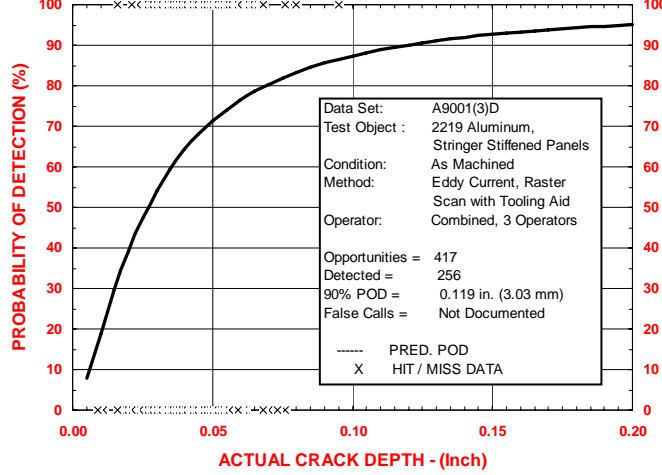


Figure 6: Example 1, Eddy Current Crack Detection on 2219 Aluminum, $\beta = 4.9/\text{in}$

In Fig. 6, crosses on the $\text{POD} = 0$ (missed flaw) and $\text{POD} = 100$ (detected flaw) levels indicate individual NDE outcome data points. The curve is a plot of $\text{POD}(a)$. $a_{90/50} = 0.119 \text{ in}$. Table 2 gives all parameters used in CMA calculations and results. Both short ($a_0 = 0$) and regular formulas were used. There is a good agreement between a_d and a_{d0} ($a_0 = 0$).

a_0, in	a_{100}, in	n for a_0	n for a_{100}	K_l	K_u	a_d, in	$a_d(a_0=0), \text{in}$
0.016	0.095	5	8	0.45	0.31	0.129	0.129
0.009	0.095	11	8	0.24	0.31	0.129	0.129

Table 2: CMA Analysis of Data in Example 1

In the above example, the margin Δ_1 is positive ($0.010''$) and reasonable ($\geq 10\%$), therefore we can claim that the CMA has demonstrated its utility for this instance. The value of j is 0.5 in above calculations. With $j = 1$, another 8% increase is observed in the estimate of a_d .

Example 2

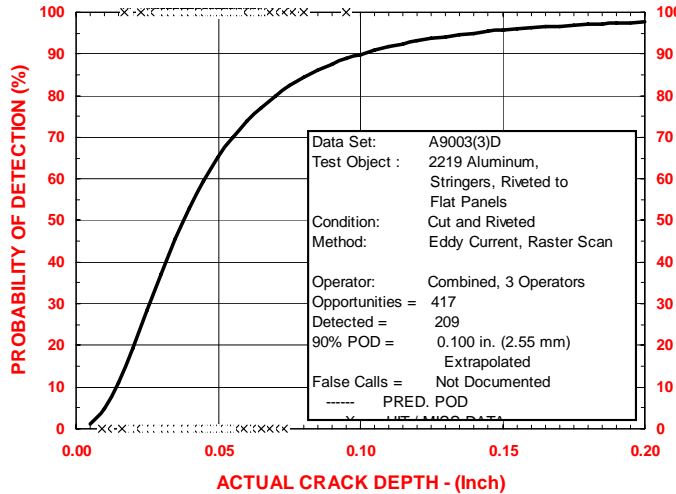


Figure 7: Example 2, Eddy Current Crack Detection on 2219 Aluminum, $\beta = 8.97/\text{in}$

a_0, in	a_{100}, in	n for a_0	n for a_{100}	K_l	K_u	a_d, in	$a_d(a_0=0), \text{in}$
0.017	0.086	13	8	0.2	0.31	0.113	0.117

Table 3: CMA analysis of data in Example 2

In example 2 (Fig. 7), the value of j is 0.5. There is a good agreement between the $a_{90/50}$ and the estimated flaw detectability a_d . The margin Δ_1 is positive (between 0.013" to 0.017") and reasonable ($\geq 10\%$), therefore we can claim that the CMA has demonstrated its utility for this instance. There is a good agreement between a_d and $a_d(a_0 = 0)$. With $j = 1$, another 8% increase is observed in a_d .

We can use the same dataset and by changing the sample size n, calculate many other CMA estimates and corresponding conservative margin. The magnitude of j influences the magnitude of the conservative margin Δ_1 . On the other hand, the exercise can be used to optimize the value of j (for a given β defined later) to obtain a desired minimum conservative margin.

POD Parameter B and Slope β

In order to quantify upper knee in the $\text{POD}(a)$ curve, a POD parameter B is defined.

$$B = 2 - \log_{10}(100 - \hat{p}\%), \quad (28)$$

where, $\hat{p}\% = \text{POD}(a)$ expressed as a % value.

B is plotted in Fig. 8 for many NDE outcomes data sets from NTIAC⁴. A value of B equal to 1 corresponds to $\text{POD}(a)$ of 90%. B equal to 1.62 corresponds to $\text{POD}(a)$ of 97.6% identified as the upper point in the range of upper knee in $\text{POD}(a)$. Similarly, a value of B equal to 2 corresponds to $\text{POD}(a)$ of 99% and so on. Thus, B is the $\text{POD}(a)$ expressed on a logarithmic scale. It allows a close look at the upper knee. We are interested in the slope of the POD parameter at $\text{POD}(a)$ of 90%. The slope is given by β .

$$\beta = \frac{\Delta B}{\Delta a} \quad (29)$$

Here we notice that as the slope β decreases, the knee becomes less sharp. A value of β at $\text{POD}(a)$ of 90% ($\beta_{90/50}$) of about 5 per inch or higher provides a sharp knee in the $\text{POD}(a)$ curve to enable use of the CMA. Data sets A9001(3)D, A9002(3)D and A9003(3)D meet this condition. The remaining datasets have shallow upper knees and the CMA is not applicable. We did not investigate lower limit of the β that still qualifies as an indicator of sharp upper knee in the $\text{POD}(a)$ curve. Note that $\text{POD}(a)$ curves for data sets A9001(3)D ($\beta = 4.9/\text{in}$) and A9003(3)D ($\beta = 8.97/\text{in}$) have been plotted in Figs. 6 and 7 respectively.

Comparing the two examples, we observe that the a_d estimate for the higher β value dataset is more conservative for the same values of j . Thus, a value of j can be obtained by trial and error by demonstrating a minimum desired amount of conservative margin Δ_1 on many flaw detectability estimates a_d from previously acquired applicable POD datasets with similar β values. This implies that the β value, the conservative margin, and the j value are interrelated and if the β value can be estimated approximately, conservative margin can be controlled by choosing a proper j value.

Estimating the β Value

Examining the B curves in Fig. 8, we infer that it is desirable to have a smaller flaw detectability size to achieve a high β value. It is also observed that for NDE techniques that can detect small flaw sizes, the range r_p is smaller too. Thus, less sensitive NDE techniques may not be good candidates for CMA. This fact is consistent with the general approach of NDE practitioners of using a very sensitive NDE technique even if the requirement flaw size is much larger so that the NDE flaw detectability can be quoted by simply multiplying the demonstrated flaw detectability (on a small sample size) by a factor of about 2. From NTIAC data sets, it is observed that for datasets, where r_p is about same as $a_{90/50}$, the following condition is true in most cases.

$$\beta_{90/50} < \frac{1}{a_{90/50}} . \quad (30)$$

Therefore, a judgment on the value of β based on a_{100} , signal to noise (S/N) ratio or contrast to noise (C/N) ratio at a_{100} or anticipated a_d can be made after taking into consideration the similarity of the NDE application to one with known $a_{90/50}$ or β . Thus, the slope β can be used as a measure of similarity between the application for estimation of flaw detectability and another similar application with established $POD(a)$ curve. The qualification of the β value and j value then allows use of the CMA formulas to compute the flaw detectability.

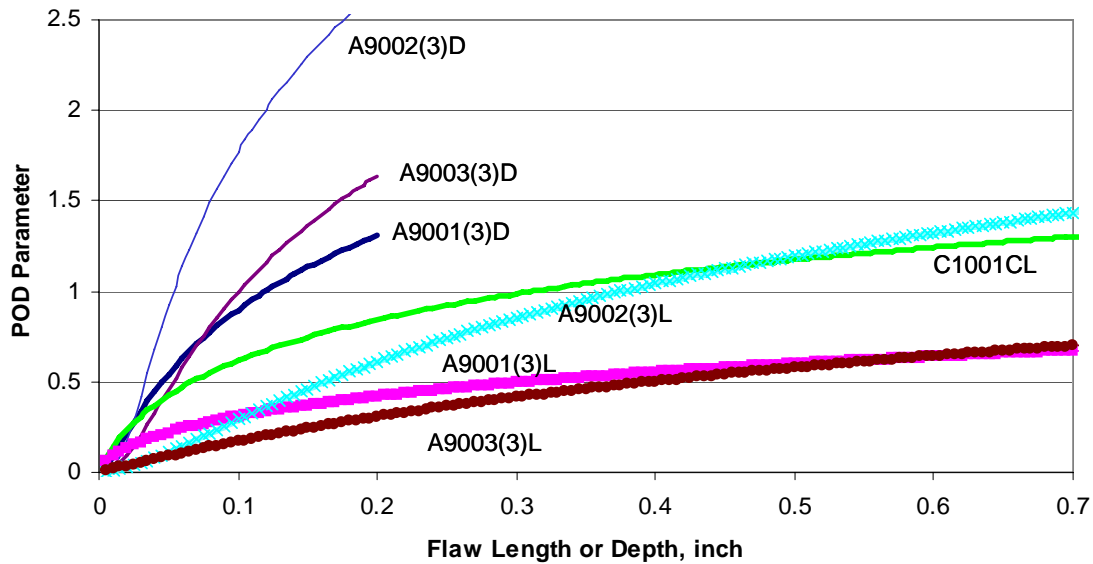


Figure 8: POD Parameter for Many Data Sets

Practical Considerations for CMA

Size a_{100} can be initially determined as a size of the largest flaw missed. Later we need to find “n” data points that support the a_{100} value. We may have to increase the value of a_{100} so that the chosen value of a_{100} is mode or the largest value of the selected contiguous data points in a narrow range with 100% detection. Similarly, the size of a_0 can be initially determined as the size of the smallest flaw detected. Later we need to find “n” data points that support the a_0 value. We may have to decrease the value of a_0 so that the value of a_0 is either mode or the smallest value of the selected contiguous data points with 0% detection.

Since the CMA estimate does not provide a quantitative confidence, it is necessary to corroborate a high confidence based on other indicators such as minimum S/N ratio (e.g. 3:1) or C/N ratio for the flaw size a_d .

The following steps are proposed to use CMA. Typically a requirement flaw size a_r is the starting point. Next, the NDE practitioner chooses an NDE method/technique that belongs to a family of techniques with regular POD datasets with high β slopes, acceptable goodness of fit measure, and successful CMA validation. The selected method has enough sensitivity (and desirable minimum S/N ratio) to demonstrate 100% flaw detection on flaws smaller than a_r such that $a_{100} < a_r/2$. The β slope is estimated based on the similarity and a value of j is chosen based on documented validation to provide a minimum conservative margin for the estimated β . If larger estimates of a_d are acceptable, then there is no need to choose optimized value of j . Instead $j=1$ may suffice. a_d is computed and minimum S/N (or C/N) ratio is measured or estimated for this flaw size and to verify that the S/N (or C/N) ratio requirements are met.

Conclusion

In this paper, we proposed an approach called the conservative margin approach (CMA) to estimate flaw detectability size when the flaw sample size is small and a rigorous POD estimation is not practical. The CMA approach, as presented here, can not provide quantitative confidence on the flaw detectability estimation. However, the CMA approach seeks to establish a flaw detectability size that is larger than the unknown $a_{90/50}$ by a certain margin. The CMA estimate is obtained by adding a margin m to the demonstrated size a_{100} . The margin m is higher if the Binomial confidence in the size a_{100} is lower.

Published POD data from NTIAC data book was used to calculate the CMA flaw size a_d and was compared with the published $a_{90/50}$. The comparison indicated that the CMA estimates are in good agreement with $a_{90/50}$ as desired and are on the conservative side as desired. The CMA approach is validated based on establishing the desired minimum conservative margin on an applicable similar POD dataset. The CMA approach does not work on techniques that are backed by irregular data where some data points indicate missed flaws for sizes much larger than $a_{90/50}$. The approach is attractive to the NDE practitioner who is often faced with the prospect to provide NDE flaw detectability size on specific applications based on limited availability of NDE outcomes data. A thumb rule of quoting the flaw detectability as double of the observed flaw detectability may not meet flaw detectability requirements. CMA may provide a better approach in these situations if CMA requirements are met. One of the key conditions includes the existence of a sharp upper knee for the $POD(a)$ curve which is assumed in the CMA based on similarity to the other applicable $POD(a)$ data. Currently, the CMA model is intended to estimate flaw size $a_{90/50}$. In future, we intend to refine the model to explore possibility of its application to estimating the flaw size $a_{90/95}$.

Acknowledgements

The author recognizes contribution by Willard Castner, NASA Johnson Space Center and Michael Suits, NASA Marshall Space Flight Center in reviewing this paper and providing valuable suggestions.

References

1. UDRI POD Software, Copyright 2000 the University of Dayton.
2. MIL-HDBK-1823, "Non-Destructive Evaluation System Reliability Assessment," 30 April 1999.
3. Berens, A. P., "NDE Reliability Data Analysis," ASM Metals Handbook, Volume 17, 9th Edition: Nondestructive Evaluation and Quality Control, ASM International, Materials Park, Ohio, 1988, pp.689-701
4. Nondestructive Evaluation (NDE) Capabilities Data book, Nondestructive Testing Information Analysis Center (NTIAC), Texas Research Institute Austin, Inc, Nov. 1997



Applicability of a Conservative Margin Approach for Assessing NDE Flaw Detectability

Ajay M. Koshti
NASA Johnson Space Center

April 19, 2007

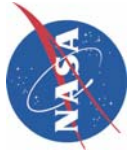
Background



NDE Flaw Detectability

- In performing NDE on components, there is a need to estimate NDE flaw detectability
 - The requirement is to detect flaws larger than or equal to a specified flaw size or the requirement flaw size, a_r
- Conventional Estimate of NDE Flaw Detectability
 - Probability of Detection $POD(a)$ curve fit method is considered to be the conventional approach. The minimum detectable flaw size is given by $a_{90|95}$ signifying 90% POD with lower 95% confidence
 - The method is statistical in nature and requires flaw detection data from a relatively large number of flaw specimens.
- Need for an alternate approach to estimate NDE Flaw Detectability with smaller number of flaw specimens
 - In many circumstances, due to the high cost and the long lead time it is impractical to build a large number of flaw specimens that is required by conventional POD methodology
 - A non-POD approach is acceptable if a high flaw detectability (e.g. 90%) with high confidence (equivalent to 50% or 95%) can be established.
 - In some cases such as class 2 hardware, the strict 90/95 flaw detectability is not required. A 90/50 flaw detectability/confidence may be acceptable

Objective and Outline



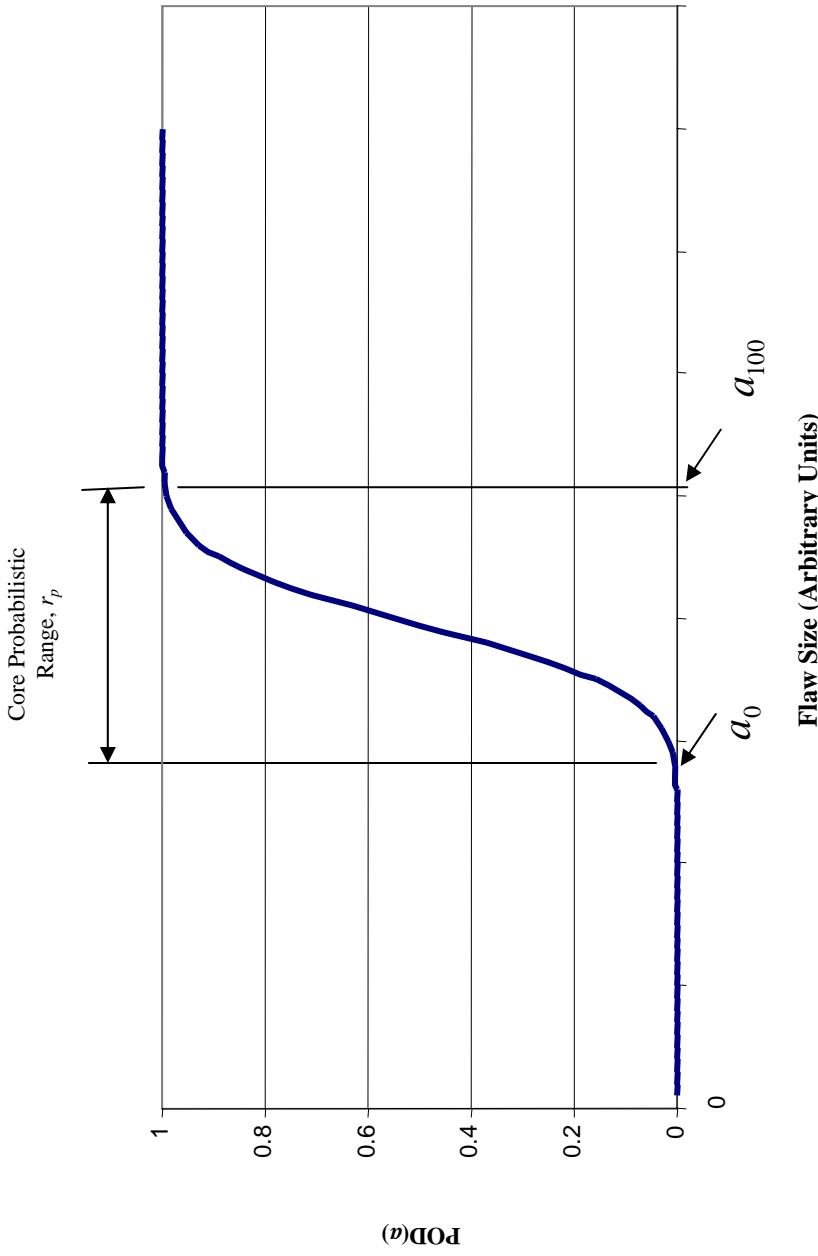
- This paper proposes a non-POD approach called the **conservative margin approach (CMA)**
 - The method uses a smaller number of flaws to establish flaw detectability size a_d
 - The flaw detectability is based on a straight line modeling of the $POD(a)$ curve (not truly non-POD)
 - The flaw detectability size a_d is compared with flaw size $a_{90/50}$ but not with $a_{90/95}$ at this point. Therefore, the flaw size a_d is considered to be an estimate of $a_{90/50}$.
- Develop the CMA model
 - CMA assumptions
- To investigate the applicability of the CMA
 - NDE flaw detectability size determined by the CMA and POD approaches have been compared on actual datasets.
- CMA Validation
- CMA Procedure
- Discuss applicability of the CMA and Conclusion

CMA Assumptions



- The CMA approach can be validated based on **similarity** with an application with existing POD (a) data.
 - The validation is based on a certain family or group of NDE applications (e.g. Surface eddy current on metallic parts with specific conditions)
- We assume certain distribution properties for the CMA approach based on the **similarity** of NDE application to be considered for CMA with an NDE application with known POD curve and successful CMA validation,
 - The distribution is assumed to be regular, i.e. no outlier data points
 - No flaws that are much larger than the $a_{90/50}$ are missed
 - a_{100} is clearly identifiable
 - Sharp upper knee i.e. the slope of the $POD(a)$ at 90% point is high ($\beta \geq 5$)
 - $POD(a)$ increases with flaw size
 - Does not assume actual POD but the NDE capability of the application is understood in terms of signal to noise (s/n) ratio or contrast ratio (c/n) on flaws of concern
 - Flaw size a_{100} can be demonstrated based on an actual NDE outcomes data with acceptable signal to noise ratio or contrast
 - Minimum 5 flaws are recommended at size a_{100}
 - Flaw/material conditions in the flaws used for demonstration are understood and considered to be the constraints under which the CMA estimate is valid.

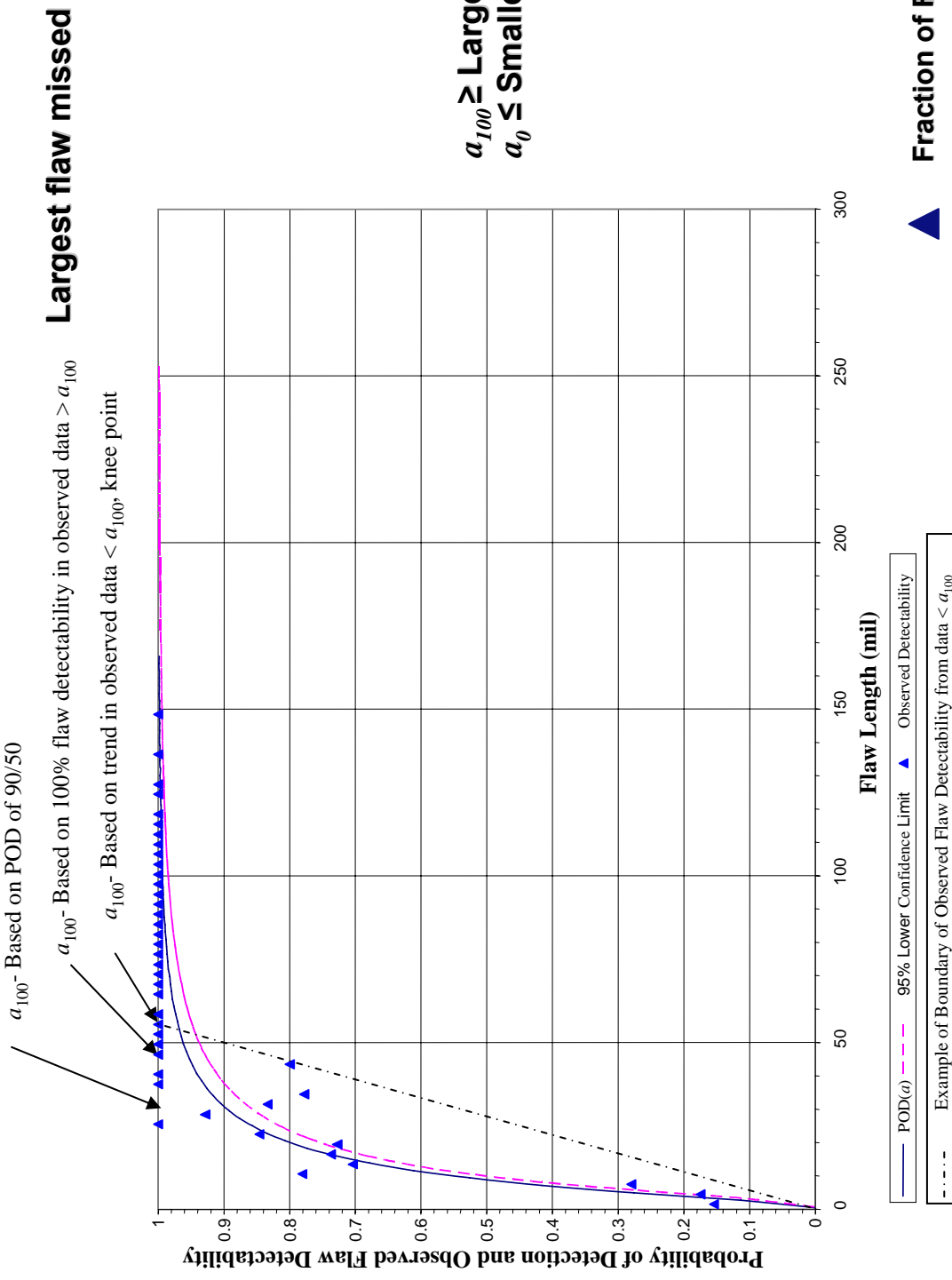
Schematic of a $POD(a)$ Curve with a Sharp Knee Bends



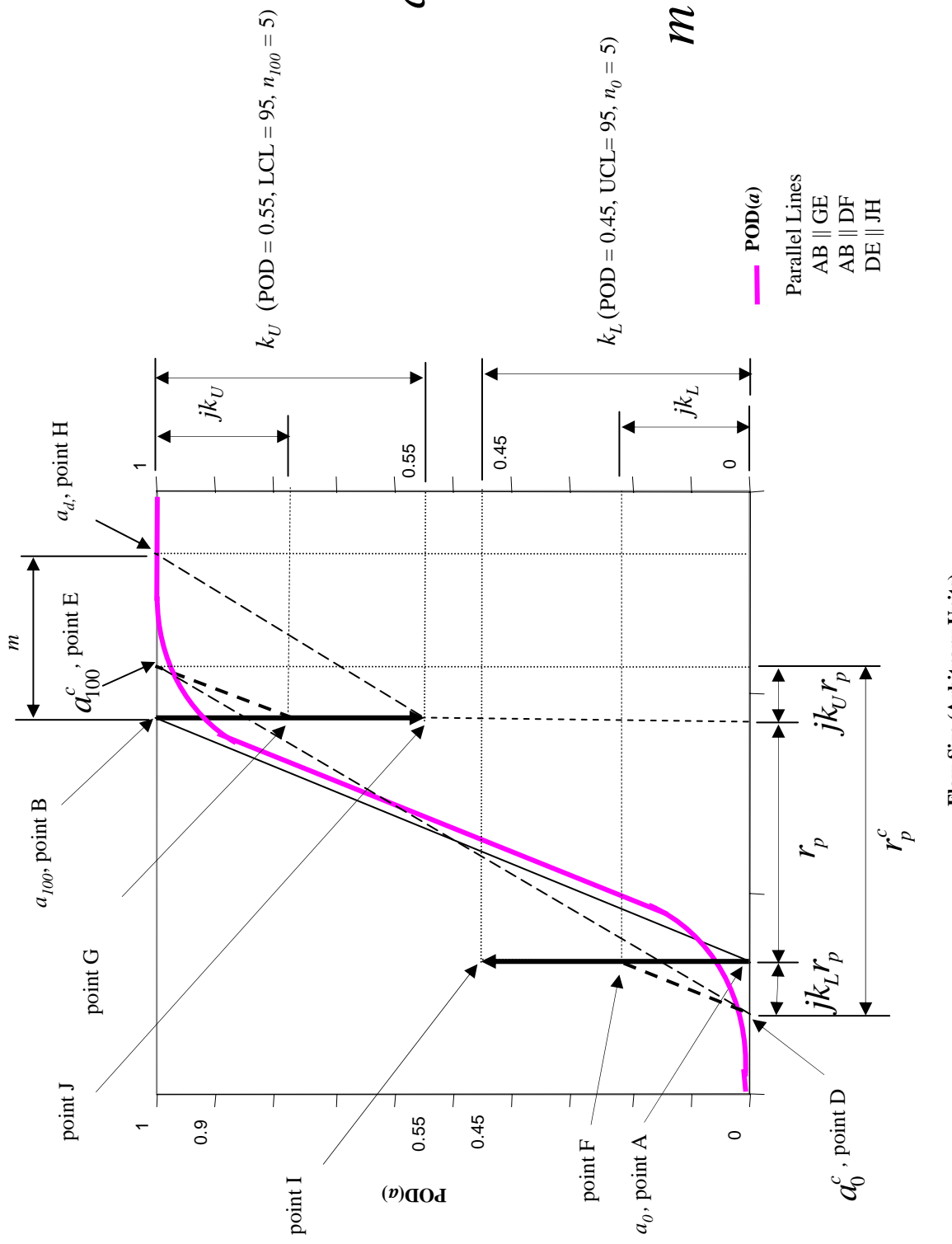
a_0 = **Smallest flaw detected**
 a_{100} = **Largest flaw missed**

POD(a) is the best fit curve with goodness of fit measure on a CMA compatible POD data

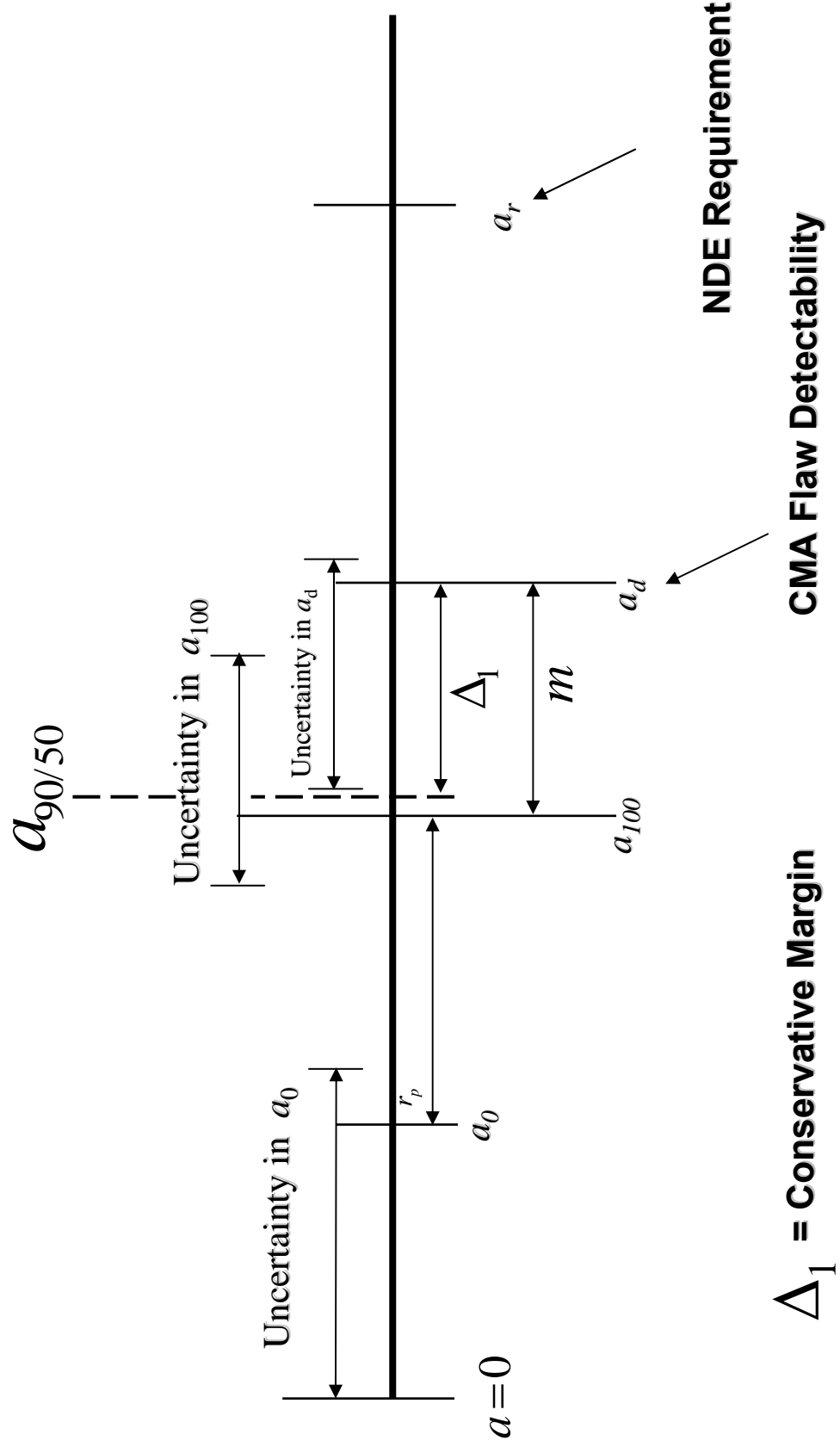
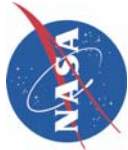
Concept of a_{100}



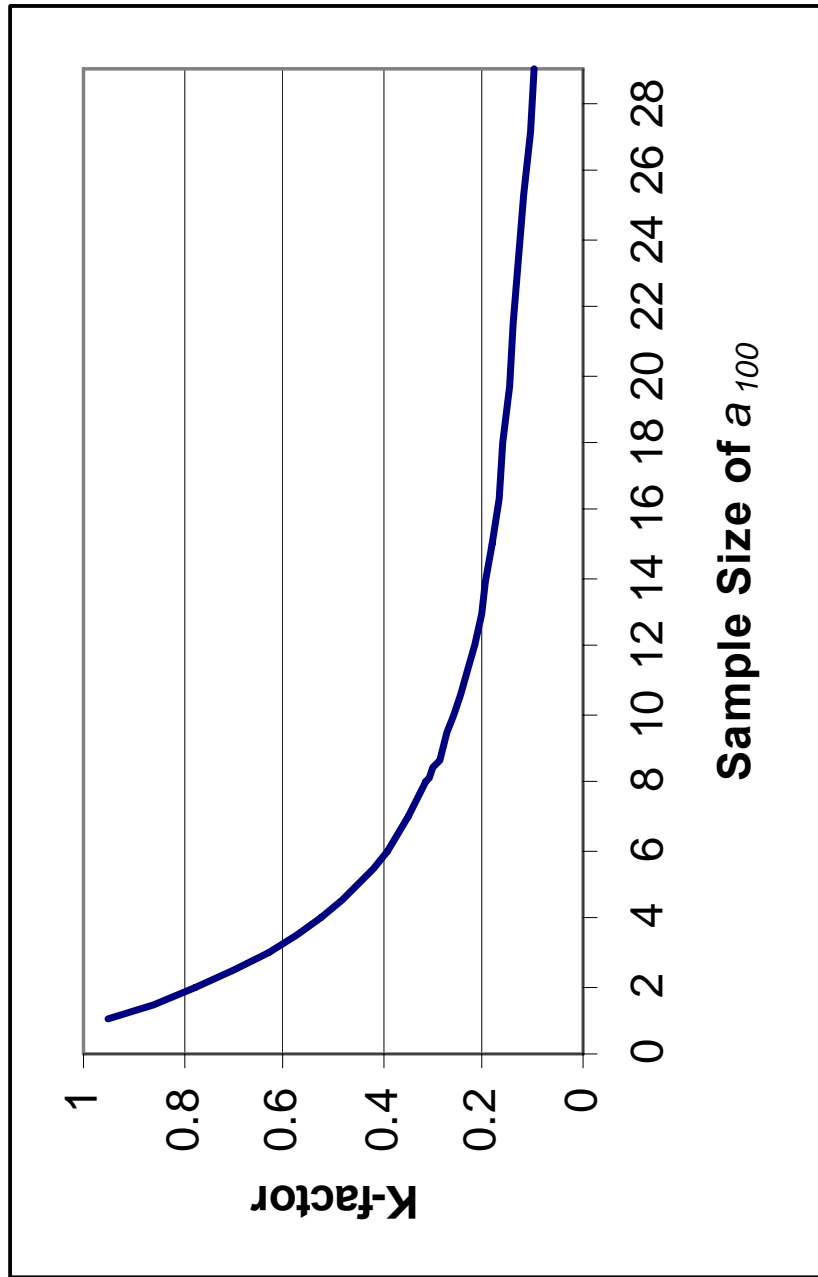
Concept of CMA



Flaw Detectability Measures



K-factor



$$k_U = 1.0 - \hat{p}_L \text{ where, } \frac{n}{n} = 1.0 \quad \text{and LCL} = 95\%$$

$$\hat{p}_L = \text{Binomial probability}$$

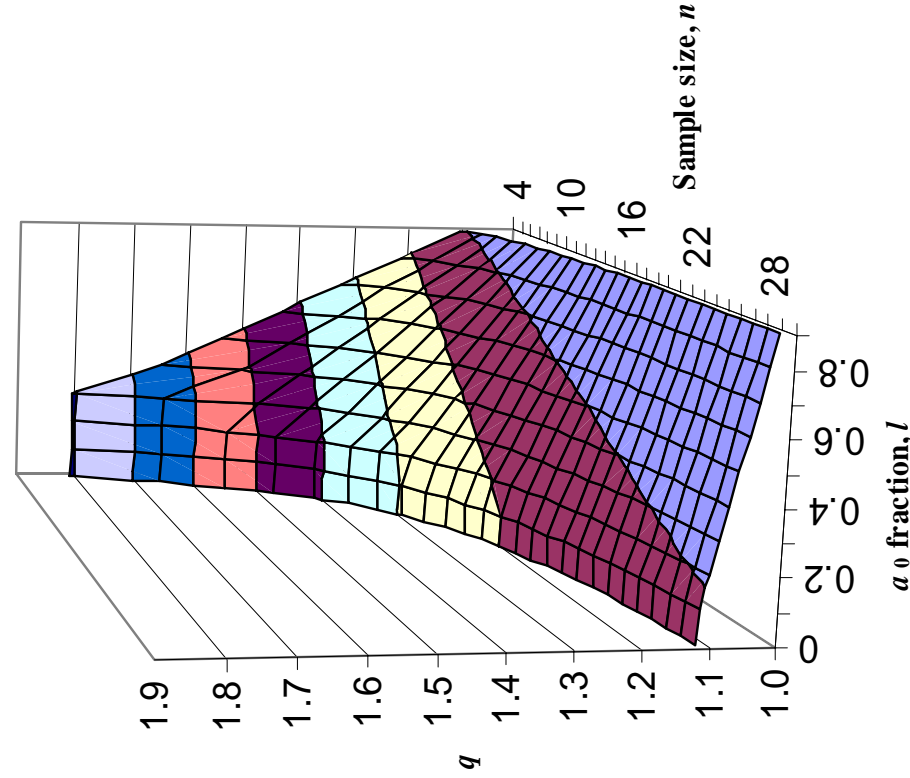
Multiplier q

n	K-factor	$q (j = 0.5)$	$q (j = 1)$
4	0.53	1.67	1.81
5	0.45	1.33	1.65
6	0.39	1.27	1.55
7	0.35	1.24	1.47
8	0.31	1.21	1.41
9	0.28	1.18	1.36
10	0.26	1.16	1.32
11	0.24	1.15	1.29
12	0.22	1.13	1.27
13	0.20	1.12	1.25
14	0.19	1.11	1.23
15	0.18	1.11	1.21
16	0.17	1.10	1.20
17	0.16	1.09	1.19
18	0.15	1.09	1.18
19	0.15	1.08	1.17
20	0.14	1.08	1.16
21	0.13	1.08	1.15
22	0.13	1.07	1.14
23	0.12	1.07	1.14
24	0.12	1.07	1.13
25	0.11	1.06	1.12
26	0.11	1.06	1.12
27	0.11	1.06	1.12
28	0.10	1.06	1.11
29	0.10	1.06	1.11

Multiplier q

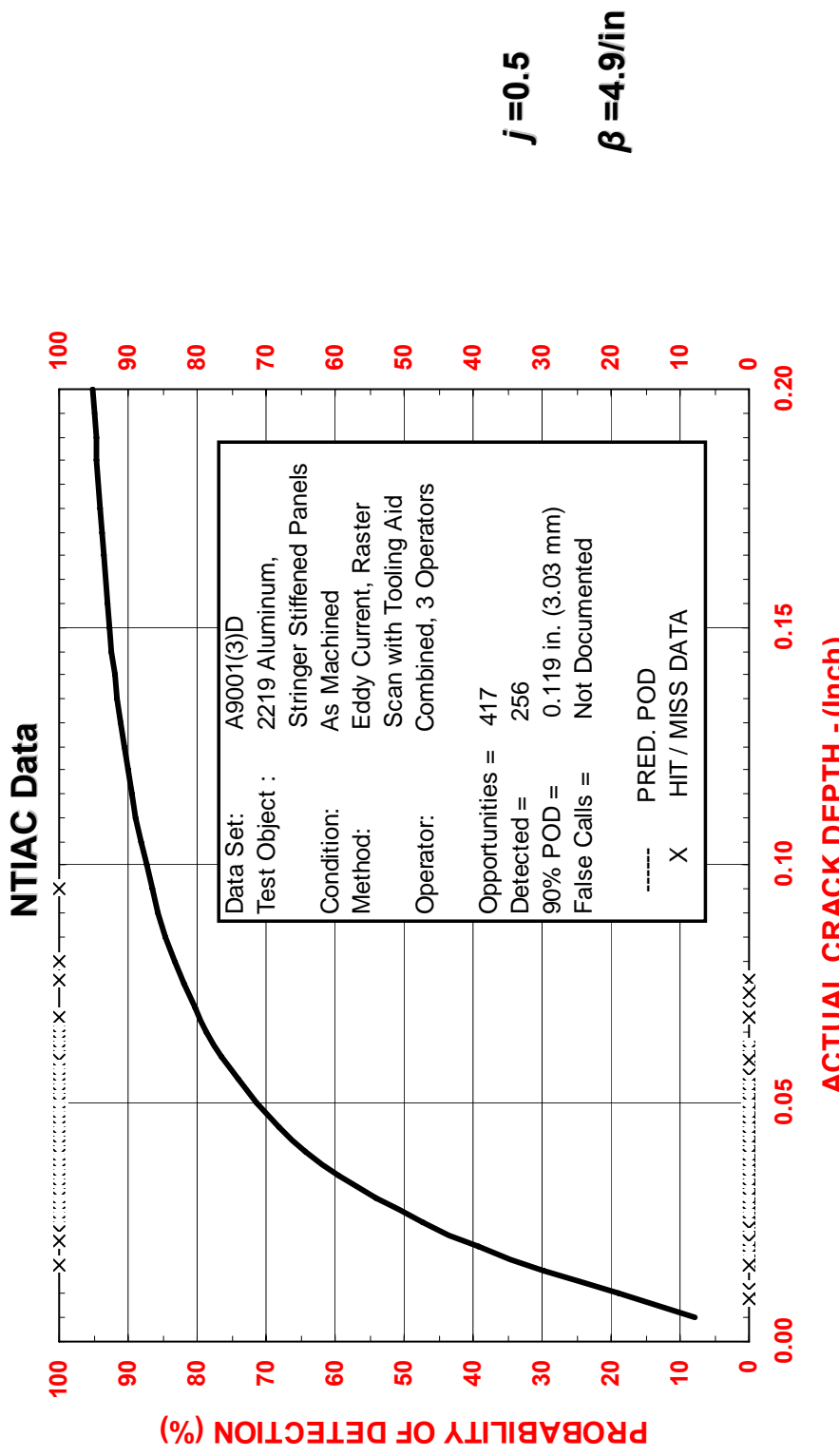
$$a_d = qa_{100}$$

$$l = \frac{a_0}{a_{100}}$$



$j \geq 0$, Higher values of j increase conservatism in the margin

Example 1: Comparison of $POD(a)$ and Ideal CMA

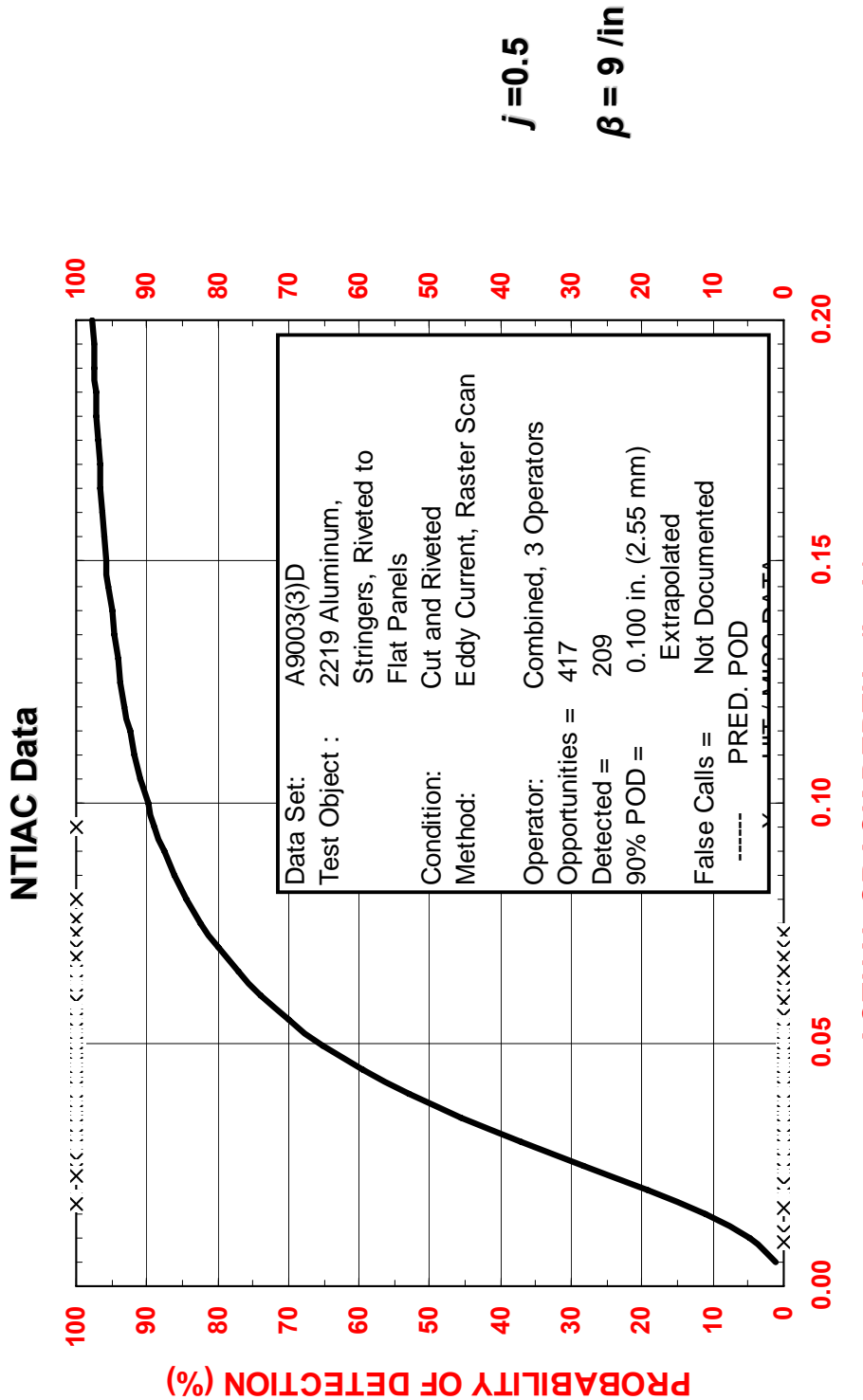


$a_0, \text{ in}$	$a_{100}, \text{ in}$	n for a_0	n for a_{100}	K_1	K_u	$a_d, \text{ in}$	$a_d (a_0=0), \text{ in}$
0.016	0.095	5	8	0.45	0.31	0.129	0.129
0.009	0.095	11	8	0.24	0.31	0.129	0.129

Ideal CMA: a_{100} is determined from NDE outcomes dataset used in $POD(a)$ analysis

The comparison may be used as part of the CMA Validation

Example 2: Comparison of $POD(a)$ and Ideal CMA

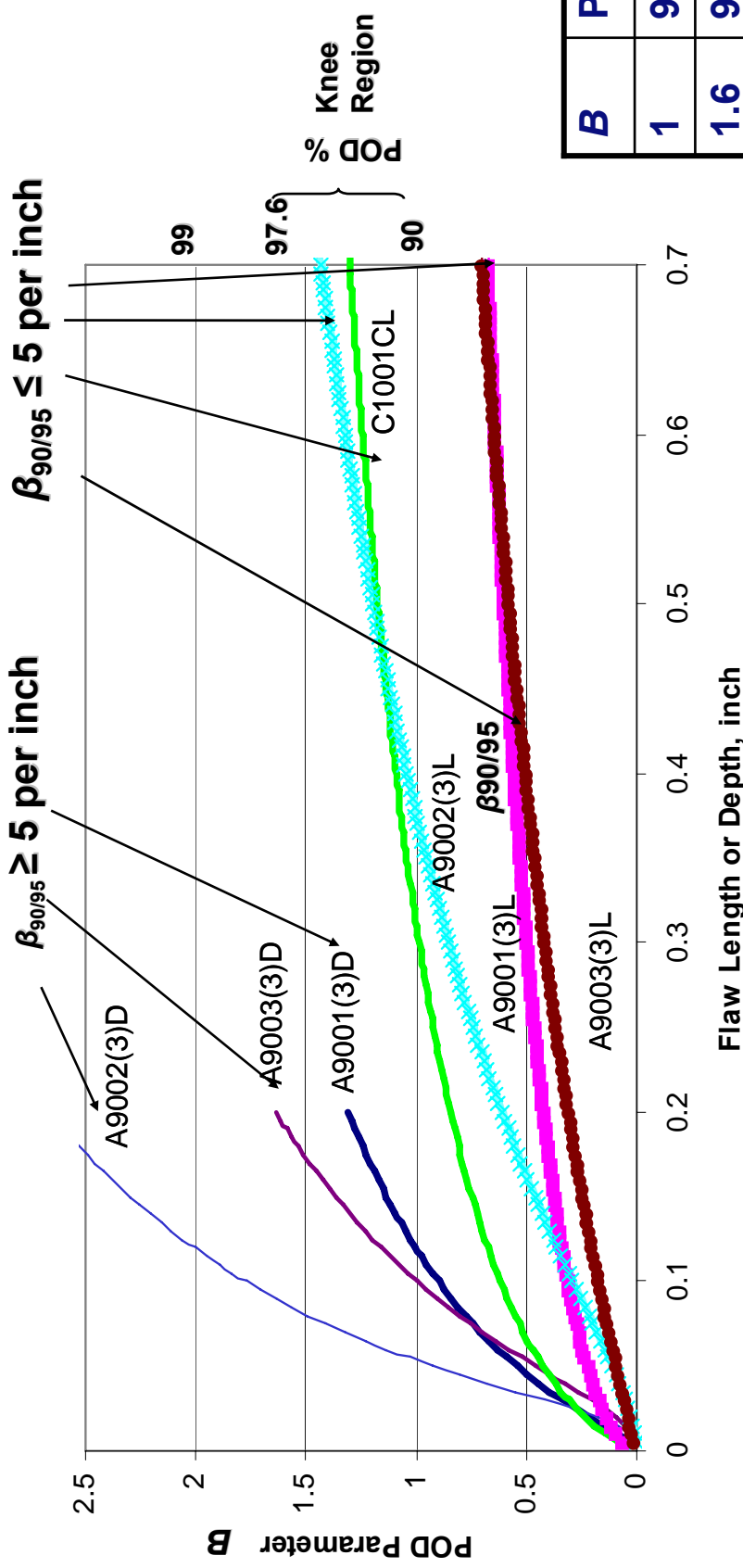


a_0 in	a_{100} in	n for a_0	n for a_{100}	K_1	K_u	a_d in	a_d ($a_0=0$) in
0.017	0.086	13	8	0.2	0.31	0.113	0.117

Ideal CMA: a_{100} is determined from NDE outcomes dataset used in $POD(a)$ analysis

The comparison may be used as part of the CMA Validation

POD Curve Plotted as POD Parameter B



B	POD(a)
1	90%
1.6	97.6%
2	99%
3	99.9%

$$B = 2 - \log_{10}(100 - \hat{P}_{\%}) \quad \beta = \frac{\Delta B}{\Delta a} \quad \beta < \frac{1}{a_{90/95}}$$

CMA may be applicable if β (at POD = 90) ≥ 5 per inch
Larger β value needs smaller value of j to provide the same percentage conservative margin.

CMA Validation



- **CMA Validation**
 - Analyze many applicable existing POD datasets of applicable NDE techniques using CMA
 - Examine if the dataset meets the CMA requirements of “regular” dataset (a_{100} can be clearly identified)
 - Compute value of slope β from the POD(a) curve. Examine if β requirements are met.
 - Choose a conservative margin Δ_1 .
 - Margin is related to β and j values
 - Determine values of j by trial-and-error to provide the minimum desired conservative margin on many possible estimates of CMA on the dataset.
 - If the desired conservative margin is demonstrated, then the dataset is CMA compatible.
 - Study similarity factors that can be used to define a family of NDE techniques that the technique under study should belong to
 - Identifying characteristics of a family of successful CMA compatible techniques is useful in assuming properties of the NDE technique at hand as same as that belonging to the applicable family of NDE techniques.

CMA Procedure



- Following steps have been proposed to use CMA
 - Typically a requirement flaw size a_r is the starting point.
 - Next, the NDE practitioner chooses an NDE method/technique that belongs to a family of techniques with regular POD datasets with high β slopes, acceptable goodness of fit measure and successful CMA validation.
 - The selected method has enough sensitivity (and desirable minimum S/N ratio) to demonstrate 100% flaw detection on flaws smaller than a_r , such that $a_{100} < a_r/2$.
 - The β slope is estimated based on the similarity to a validated family of NDE techniques and a value of j is chosen based on the documented validation within the chosen family of techniques to provide a minimum conservative margin for the estimated β .
 - If larger estimates of a_d are acceptable, there is no need to choose optimized value of j . Instead $j=1$ may suffice. a_d is computed and minimum s/n (or c/n) ratio is measured or estimated for this flaw size and to verify that the s/n (or c/n) ratio requirements are met.

Conclusion



- In this paper, we proposed an approach called the **conservative margin approach (CMA)** to estimate flaw detectability size when a large sample size and a rigorous POD estimation is not practical.
- CMA model is validated on similar datasets before it is used for the application at hand.
- The CMA approach seeks to establish the flaw detectability size that is larger than the unknown $a_{90/50}$ by a certain margin.
- The margin between the flaw size a_d and a_{100} is higher if the confidence in size a_{100} is lower.
- Published POD data from NTIAC databook was used to calculate the ideal CMA flaw size a_d and compare it with the published $a_{90/50}$
 - The comparison indicated that the CMA estimates are on conservative side as desired. The CMA approach may provide margins as high as a_{100} from the demonstrated size a_{100} depending upon the number of datapoints in the NDE trials test.
 - The CMA approach does not work on NDE techniques that result in irregular data where some datapoints indicate missed flaws for sizes greater than $a_{90/50}$ or when $\beta_{90/50} < 5$ per in.
 - The approach is attractive to the NDE practitioner who is often faced with prospect to provide NDE flaw detectability on specific applications based on a limited availability of data. If flaw detectability requirements do not need strict 90/95 detection and reliability, CMA may be a good candidate.
 - The novelty of CMA approach is that it uses previously acquired data on similar applications for prediction of flaw detectability size of a new NDE application.